Experimental predictive control of the infrared cure of a powder coating: a non-linear distributed parameter model based approach

Isabelle Bombard, Bruno da Silva, Pascal Dufour, Pierre Laurent

1
Université de Lyon, Lyon, F-69003, France; Université Lyon 1;
CNRS UMR 5007 LAGEP (Laboratoire d'Automatique et de GEnie des Procédés),
43 bd du 11 novembre, 69100 Villeurbanne, France
Tel +33 (0) 4 72 43 18 45 - Fax +33 (0) 4 72 43 16 99
http://www-lagep.univ-lyon1.fr/ http://www.univ-lyon1.fr http://www.cnrs.fr

Experimental predictive control of the infrared cure of a powder coating: a non-linear distributed parameter model based approach

I. Bombard[1], B. Da Silva, P. Dufour[2] and P. Laurent
Université de Lyon, F-69622, Lyon, France;
Université Lyon 1, Villeurbanne;
CNRS, UMR 5007, LAGEP.
43 bd du 11 novembre, 69100 Villeurbanne, France

This paper deals with the experimental model based predictive control of the infrared cure cycle of a powder coating. It is based on a dynamic infinite dimensional model of the cure in one spatial domain, which aims to represent the evolution of the temperature and the degree of cure during the cure under infrared flow. The sensitivity of this model with respect to the main radiative property is experimentally highlighted under open loop conditions. This partial differential equation model is then approximated in finite dimension in order to be used by the predictive controller. Since the sampling time is small (one second), a special model predictive control formulation is used here, which aims to decrease the on-line computational time required by the control algorithm. Experimental evaluation of this controller that is based on the MPC@CB software is then presented. For black and white paintings, the robustness of this control algorithm is shown during an experimental temperature constrained trajectory tracking, even under a strong modeling uncertainty. The conclusion of this study is that this controller may be used for advanced control of powder coating cure.

Keywords: Process control, powder coating, optimization, radiative curing, model predictive control, heat transfer.

1. Introduction to powder coatings

Powder coatings used in coating techniques are finely ground plastic particles consisting of resin, cross linker (in thermoset powders), pigments & extenders, and various flow additives and fillers to achieve specific properties. They are principally based on epoxy, polyester, hybrid (combinations of acid polyester and epoxy) and polyurethane resins. Generally they are either thermoset or thermoplastic coatings, but quite recently ultra-violet curable coatings (where the reaction is initiated by ultra-violet (UV) radiation) and low-temperature coatings designed for heat sensitive substrates have appeared on the coatings market. During the cure, most generally realized under infrared emitters, thermoset powder coatings are present with a broad variety of morphologies (Lee et al., 1999; Véchot et al., 2006):

- at the powder state, they are applied on the steel panel (the substrate) by electrostatic means; the packing of the grains as well as the thickness of the powder layer can be variable and each powder can present different particle size distributions;
- the curing begins with the melting of the powder coating, which is (at this state) like a viscous liquid;
- after a viscosity decay due to the temperature increase during the cure, the polymerization reaction begins and the surface structure builds up until the end of the reaction.

The advantages associated with powder coatings include (Weiss, 1997): durable finishes, high application efficiency, easy clean-up and recycling. Powder coatings also represent a technological solution that is environmentally friendly since these paintings are almost 100% solids (i.e., near zero VOC (Volatile Organic Compound) content). Due to VOC regulations, powder coatings (as waterborne coatings) could therefore replace organic solvents in coating

techniques. Although they can be a mean to decrease VOC pollution, they have yet not found the success they deserve and their application domains remain unchanged: architecture (outdoor and indoor), furniture, domestic appliances, heaters, cars accessories (Véchot et al., 2006). The main issue is dealing with the cure cycle of the powder coatings. Indeed, during the cure of powder coatings (also known as the curing or curing cycle), the quality of the cured product is strongly influenced by the temperature path together with the maximum temperature to which the powder coating is heated. Deviation from specified optimum cure conditions can therefore lead to coatings which have surface defects and/or coatings which do not adhere to the substrate. The curing cycle optimization generally depends primarily on the know how of the operator and on the use of temperature profiling software (Wood, 2007).
The PhD thesis of Bombard was a global research project on the infrared (IR) curing process of powder coatings (Bombard, 2007) aimed at bringing some technical knowledge about the experimental cure cycle of powder coating to potential users. It tackled both modeling and control aspects. The first complete model of the coating radiative properties and of the spectral emissivities of the infrared emitters may be found in (Véchot et al., 2006) and (Bombard et al, 2008). However, in this model used here, the reflectance and the emitter emissivity are not measured on-line during the curing, although they vary with the type of infrared flow emitted: any model based controller used for this process has therefore to be robust with respect to this modeling uncertainty. This model has previously been used in simulation in a closed loop control approach (Abid et al., 2007) to tune on-line the infrared flow applied during the cure cycle, such that one of the curing characteristics (the measured temperature at the bottom surface) tracks as best as possible a specified time dependant trajectory. These simulations have shown that a Model Predictive Control (MPC) based on this model gives better results than a proportional integral derivative (PID) controller when robustness with respect to model parameter uncertainty is needed. In this paper, the next step is tackled: evaluation of the robustness of this model based controller with respect to real uncertainties due to experimental conditions.
This paper is structured as follows: first, the modeling principles of the powder coating cure under IR flow are detailed. It is a non-linear partial differential equation (PDE) model in one spatial dimension. The influence of the main model parameters during the cure is underlined. Then, the model based predictive control approach is reviewed, where any constrained control objective may be specified in the control software (trajectory tracking, processing time minimization). Experimental results then help to show how the proposed special MPC algorithm may be useful and robust to experimentally control this kind of process, even if uncertainties dealing with the material used exist.

2. Modeling of powder coatings

Model based control techniques would be very helpful to get a better control of the cure (and hence get a final product of better quality) and to promote the use of powder coatings in more application domains. Meanwhile, very few models of the curing process have yet been developed in the literature:

- The first study (Degnan, 1982) dealt with the modeling of electron beam cured coatings based on an ordinary differential equation (ODE) curing model coupled with the temperature profile obtained in 2-D by non dynamic model.
- Much later, in (Deans and Kögl, 2000), a Monte Carlo model of the heat transfer process was used for the curing of powder coatings using gaseous infrared heaters, but without modeling the degree of cure.
- In (Chattopadhyay et al., 2005), an ODE model of degree of cure of moisture-cured polyurethane/polyurea coatings under a software based cure cycle was presented, and

combined with the measurement of a mechanical property. There was no heat transfer modeling.

- Vergnaud's team was the first to use PDE models: In (Perou and Vergnaud, 1997) a coupled PDE model of heat and mass transfers and cure was built to study the resistance of coil coatings to liquids.
- In (Salagnac et al., 2004), a PDE model of heat and cure of composite material parts in a small diameter autoclave was developed and validated experimentally.
- (Véchot et al., 2006) and (Bombard et al, 2008) developed the basis of the model used in this paper: it was a coupled heat transfer and cure PDE model of powder coating during infrared curing.

2.1. Parameters influencing the radiative properties

Numerous reports in the literature show how the chemical composition and physical state of materials affect the intensity and the shape of the reflectance spectra, which is an important parameter in the IR curing process:

- The cure cycle has a strong impact over the radiative properties (Carr et al., 1999); the effect of the cure is though variable, depending on the chemical composition of the powder coating. When comparing the spectral absorptivities of uncured and cured powder coatings; (Carr et al., 1999) found the largest absorptivity differences with the unpigmented coatings; for the white coatings the difference was smaller whereas the difference was insignificant for the black ones. Therefore, the knowledge of the radiative properties enables to determine their dependence with the physical and chemical state of the material and, as a consequence, is useful in numerous applications involving radiative heat transfer (Carr et al., 1999; Deans and Kögl, 2000), such as the radiative curing of powder coatings. This knowledge is yet insufficient, as the absorption of infrared energy by a material depends not only on the spectral absorption characteristics of the material being heated but also on the spectral output of the infrared source (Bombard et al., 2005; Véchot et al., 2006). This will be underlined in our study.
- The spectral output of the infrared source indeed influences the (heated) material radiative properties (Papini, 1996, 1997; Tongsuo et al., 2002, Ventura and Papini, 1999). This phenomenon is particularly more difficult to study if the infrared flow emitted is time dependant, for example if it is applied as a closed loop control action like in this work.
- Radiative properties are also influenced by the physical state of the painting: the particle size, the particle shape, the granular packing and the thickness (for powders). For films, they are function of the surface roughness and the thickness. Moreover, pigments greatly affect the infrared absorption by scattering and/or absorbing IR radiation. For example carbon black absorbs IR energy almost completely throughout the IR spectrum.
- The substrate nature and its surface state can also influence the reflectance values; the effect can be more or less important, depending on the coating thickness and the pigment nature (Tongsuo et al., 2002).

Although the efficiency of IR curing depends mostly on both the spectral emissions of the infrared source and on the coating radiative characteristics during the cure, we have not found any reference dealing with the measurement of the spectral reflectance during the cure cycle: Spectral reflectances are measured either before the cure (at the powder state) or after the cure (the cure state) (Bombard et al., 2008, Carr et al., 1999, Deans and Kögl, 2000). Reflectance values vary with the chemical composition, the pigment nature, and are influenced by the powder coatings cure. Cure cycle depends both on the coating radiative properties of the powder coating and on the kind of IR emitter used. A better knowledge of the spectral emissivities of infrared heaters and of the parameters influencing the radiative absorption of

the powder coating is therefore first needed to optimize the curing process through a model based approach.

2.2. Experimental setup

2.2.1. Material

The powder coatings selected for this work are widely used commercial thermosetting powders in the metal coating industry and are supplied by DuPont Powder Coatings France SAS. The paint used here (named paint A) is a polyester-based system containing Triglycidylisocyanurate (TGIC). It is supplied in black (B) and white (W); their characteristics and ideal curing conditions obtained from technical recommendations of Dupont powder coating France are summarized in Table 1. The substrates used for this study are steel standard test panels with dull and matte finish. They are produced by the Q. Panel Co. and supplied by Labomat. The application of the powder on the steel panel is realized with a GEMA PGC1 corona spray gun. Quasi-uniform powder layers are realized (approximate thickness is 70 µm). Thickness is measured on cured samples using a gauge and the gloss is measured after the curing with an Ericsen pico-glossmeter.

2.2.2. Equipment

2.2.2.1. Reflectance Measurement

The measurement of the total hemispherical spectral reflectance (defined as the ratio of hemispherical reflected flow from a surface and incident flow) is not performed from zero to infinite for the real spectrum, but from 1.4 µm (the near visible) to 12.5 µm (where the sensor becomes less efficient). It is based on a Bruker IFS 66vs Fourier Transform Infrared (FTIR) spectrophotometer, equipped with a Globar source and a KBr beam splitter and coupled with liquid nitrogen cooled mercury cadmium telluride (MCT) external detector:

- For dynamic reflectance measurements, resolution is set at 4 cm^{-1} and 1250 scans are co-added to improve the signal-to-noise ratio of each spectrum.
- For static reflectance measurements, resolution is set at 4 cm^{-1} and 10000 scans are co-added to improve the signal-to-noise ratio of each spectrum.

The spectrophotometer is fitted with a substitution integrating sphere, for collecting the specularly and diffusely reflected radiations. ‘Substitution’ means that there is only one port for the sample and the reference standard, and that the two samples have to be measured subsequently. Conversely, comparison spheres have two ports for sample and reference standard. The inside wall of the integrating sphere is coated with a diffuse gold coating with a nearly constant reflectance (0.9865, data from Labsphere).
The relative reflectance is defined as the ratio of the intensity reflected by the sample to the intensity reflected by the standard. The sample absolute reflectance equals the relative reflectance multiplied by 0.9865 (due to the non perfect integrating sphere).
Painting samples are placed under the sample and reference port of the sphere, and the incident radiant beam is nearly normal to the powder coating surface. The total near-normal hemispherical spectral reflectance contains both the specular and diffuse components. For dynamical measurements, samples are placed on a brass medium equipped with two heating cartridges, which enables at the same time to measure the reflectance during the cure of the powder coatings and to follow the temperature imposed by the brass medium. Reflectance measurements are made on powder coatings already deposited on steel panels, so that the reflectance measurements are made in conditions similar to those used when curing the

samples in our experimental infrared oven. Painting samples used in this work are first studied before curing (powder state), during curing (dynamic measurements) and after curing (cure state) at 190°C latter and at ambient temperature.

2.2.2.2. Experimental curing process, actuator and sensor

To evaluate the performances obtained with the proposed MPC algorithm, powder samples are cured in an experimental infrared oven (Figure 1). The upper surface of the radiator is painted in black, which enables to absorb the reflected infrared emissions; the radiator is maintained isotherm thanks to water circulation. The role of the shutter is to protect the user from dangerous radiations (only near infrared radiations are dangerous because they may contain some UV radiations). The sample holder enables the user to always put the sample at the same place thanks to a guiding rail.

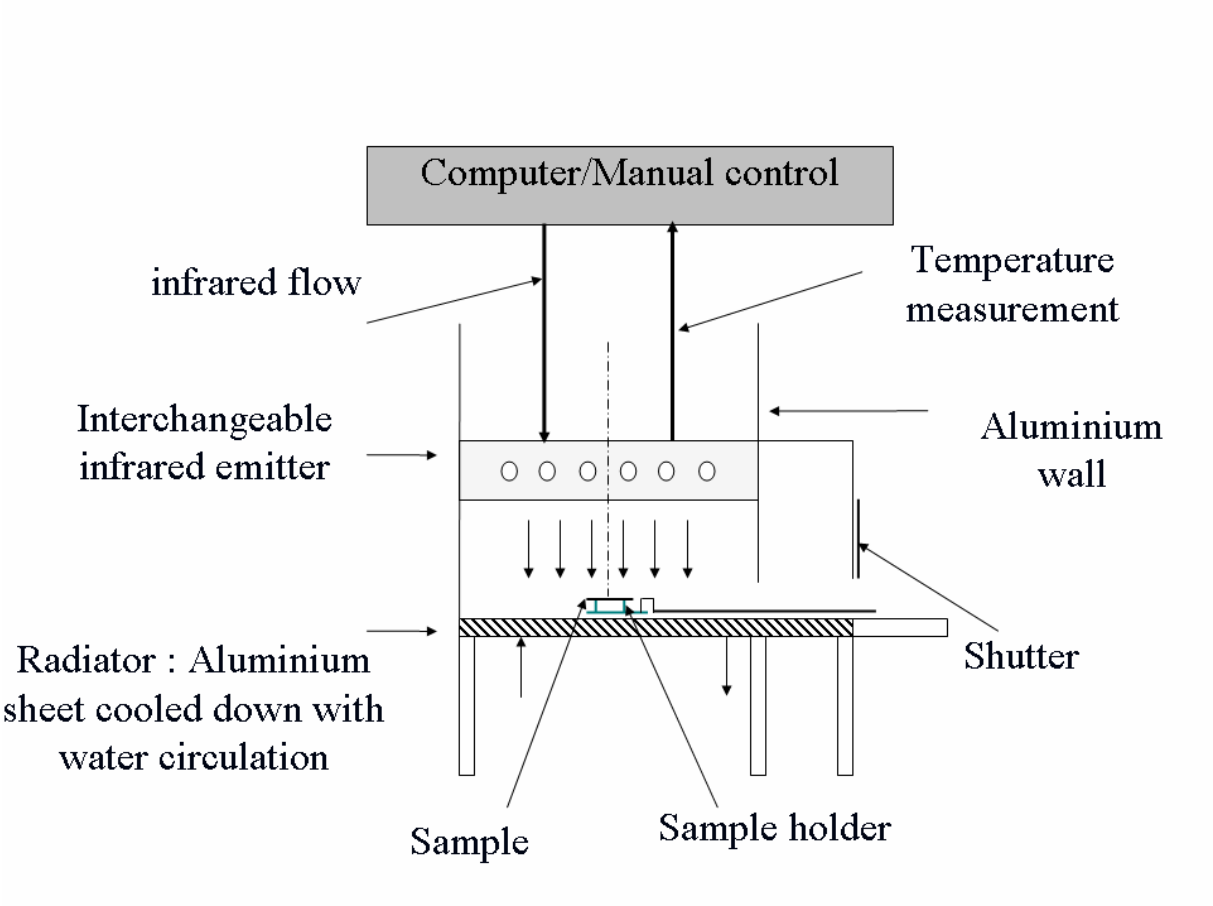

Figure 1. Experimental infrared oven.

In term of actuator, the infrared oven is fitted out with an infrared emitter having 9 interchangeable lamps. The different types of infrared sources are listed in Table 2. The value of the infrared flow applied during the cure may be tuned:

- manually;
- or kept constant in open loop;
- or computed by the controller (closed loop control).

An electronic power device provided by Eurotherm Automation[1] (TC3040), principally composed of 3 thyristors that connect the 3 phase AC power grid (ranging from 0 VAC to 230 VAC) to the lamps, controls the voltage at the connection of the lamps and hence the

value of the infrared flow emitted. The infrared flow emitted $\phi_{ir}(t)$ is controlled by the phase angle triggered gates of the AC-AC converters through the manipulated control voltage of the thyristors gate (ranging from 0V DC to 10V DC). In this study, even if the real control action is the thyristors gate voltage, the infrared flow emitted $\phi_{ir}(t)$ is considered as the manipulated control variable *u(t).*

In term of sensor available during the curing for control purpose, a temperature is measured by a type K thermocouple placed under the substrate (at the lower surface of the sample). Its sensitivity is 40 µV/ K and the uncertainty on the measure is 1K. This temperature is used as the controlled variable $y_p(t)$ in our study.

The actuator and the sensor are connected to the PC through an input/output device: It is a digital/analogical MOD-MUX module of Proconel[2]. It requires a RS485 connection with a conversion to the RS232 Modbus protocol, following the Modicon format[3].

2.3. Mathematic model and main parameter study

2.3.1 Model

The 1D thermal model used here was previously developed in (Bombard et al, 2008). It is based on the Fourier law of heat conduction and the Figure 2 shows the boundary conditions applied at the top surface of the powder (subscript *p* in the model) and at the bottom of the metallic substrate (subscript *s* in the model).

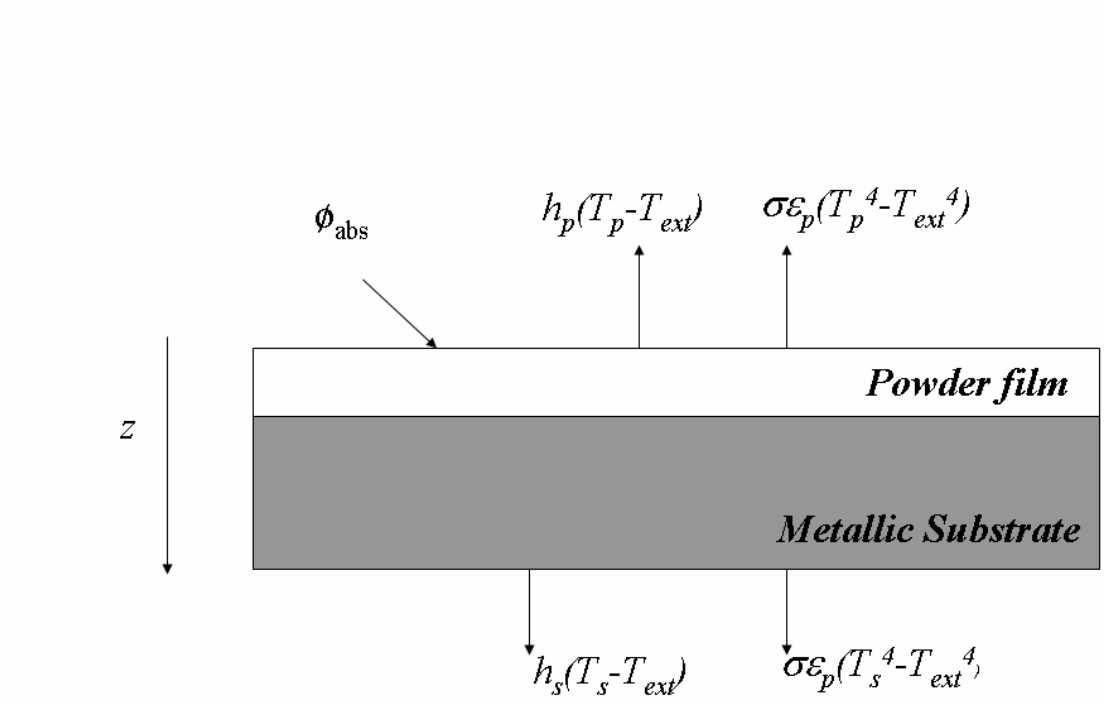

Figure 2. Schematic drawing of the “substrate and powder” sample (Bombard et al, 2008).

The thermal balance uses both the temperature variable *T(z,t)* varying during the time *t* across the thickness *z* of the powder coated metal sample (*z=0* is the top surface), and the degree of cure conversion *x(z,t)* (which ranges from 0^+ at the beginning to 1 at the end). Inside the powder, it leads to the following equation (the signification of the model parameters may be found in table 3):

$$\frac{\partial T_p(z,t)}{\partial t} = \frac{\lambda_{c,p}}{\rho_p C_{pp}} \frac{\partial^2 T_p(z,t)}{\partial z^2} - \frac{e_p \Delta H_0}{C_{pp}} k_0 e^{\left(\frac{-E_a}{RT_p(z,t)}\right)} x^m (1-x)^n \quad \forall z \in \left]0, e_p\right[, \forall t > 0 \quad (1)$$

where $T_p(z,t)$ is the temperature across the powder layer, which thickness is e_p. The thermal balance inside the metallic substrate leads to the following equation for the temperature $T_s(z,t)$ inside the substrate, which thickness is e_s:

$$\frac{\partial T_s(z,t)}{\partial t} = \frac{\lambda_{c,s}}{\rho_s C_{ps}} \frac{\partial^2 T_s(z,t)}{\partial z^2} \quad \forall z \in \left]e_p, e_p + e_s\right[, \forall t > 0 \quad (2)$$

The first boundary condition is at the top of the painting film:

$$-\lambda_{c,p} \frac{\partial T_p(z,t)}{\partial z} = \phi_{abs}(t) - \sigma \varepsilon_p (T_p(z,t)).(T_p^4(z,t) - T_{ext}^4) - h_p (T_p(z,t) - T_{ext}) \text{ at } z = 0, \forall t > 0 \quad (3)$$

where $\phi_{abs}(t)$ is the infrared flow absorbed at the surface by the sample, which depends on the manipulated variable considered: the emitted infrared flow $\phi_{ir}(t)$ (more details are given in the following).

The second boundary condition expresses the continuity of the thermal flow at the interface e_p of the powder and the substrate:

$$-\lambda_{c,p} \frac{\partial T_p(z,t)}{\partial z} = -\lambda_{c,s} \frac{\partial T_s(z,t)}{\partial z} \text{ at } z = e_p, \forall t > 0 \quad (4)$$

The third boundary condition, at the lower surface (where the temperature sensor is located), is:

$$-\lambda_s \frac{\partial T_s(z,t)}{\partial z} = -\sigma \varepsilon_s (T_s(z,t)).(T_s^4(z,t) - T_{ext}^4) - h_s (T_s(z,t) - T_{ext}) \text{ at } z = e_p + e_s, \forall t > 0 \quad (5)$$

The initial conditions for the dynamic equations (1) and (2) are:

$$T_p(z,t) = T_s(z,t) = T_{ext} \forall z \in [0, e_p + e_s], t = 0 \quad (6)$$

Concerning the degree of cure *x(z,t)* of the powder, the polymerization reaction is characterized by the Sesták-Berggren law (Sesták, 1984):

$$\frac{\partial x(z,t)}{\partial t} = k_0 e^{\left(\frac{-E_a}{RT_p(z,t)}\right)} x^m (1-x)^n \quad \forall z \in \left[0, e_p\right], \forall t > 0 \quad (7)$$

with the initial condition:

$$x(z,t) = 0^+ \forall z \in [0, e_p], t = 0 \quad (8)$$

2.3.2 Evaluation of the IR flow absorbed by the paint

The state of the system described by this non-linear PDE model depends on boundary limits and, more especially on the flow $\phi_{abs}(t)$ absorbed on the surface of the painting:

$$\begin{cases} \phi_{abs}(t) = \alpha_p(T_{surf}(t)).\phi_{ir}(t),\ t > 0 \\ T_{surf}(t) = T_p(z,t),\ \text{z=0}, t > 0 \end{cases} \quad (9)$$

with :

$$\alpha_p(T_{surf}) = \left\{ \int_0^\infty E(\lambda) \cdot \alpha_{\lambda p}(\lambda, T_{surf}) d\lambda \right\} \cdot \frac{1}{\int_0^\infty E(\lambda) d\lambda} \quad (10)$$

and :

$$\phi_{ir}(t) = FF \int_0^\infty E(\lambda) d\lambda = f(u(t)) \quad (11)$$

where $\alpha_{p(T_{surf})}$ is the absorption coefficient of the painting at the top surface, $\phi_{ir}(t)$ is the thermal radiative flow arriving on the top of paint, which is the manipulated variable of this study. $E(\lambda)$ is the spectral irradiance of the IR emitters, $\alpha_{\lambda p(\lambda, T_{surf})}$ is the spectral absorption coefficient of the painting at the surface as a function of the wavelength of the emitter lamps, and FF is the form factor used between the sample and the emitter which depends mainly on the distance between them.

2.3.3 Model parameters study

We should yet keep in mind that high temperature emitters are better to convert electrical energy in IR radiation (Carr et al., 1999), as clearly highlighted on the experimental spectral curves (Figure 3). NIR lamps are said to be high temperature emitters (T_{lamp}=2950 K for a 230V lamp voltage) whereas MWIR lamps are said to be low temperature emitters (T_{lamp}=1750 K for a 230V lamp voltage). For one type of emitter, this experimental spectral curve is used to calculate the integral terms (10) and (11). It may be noted on these curves (Figure 3) that $\alpha_{p(T_{surf})}$ fully depends on the type of the emitter (NIR, SWIR or MWIR) but also on the input voltage of the emitter lamps that modulates the IR flow emitted, as it can be seen from the 2 curves obtained with 140 V and 230 V. For the MWIR emitter, we can also remark on (Figure 3) the difference between the spectral behavior of the real emitters and the black body at the same temperature.

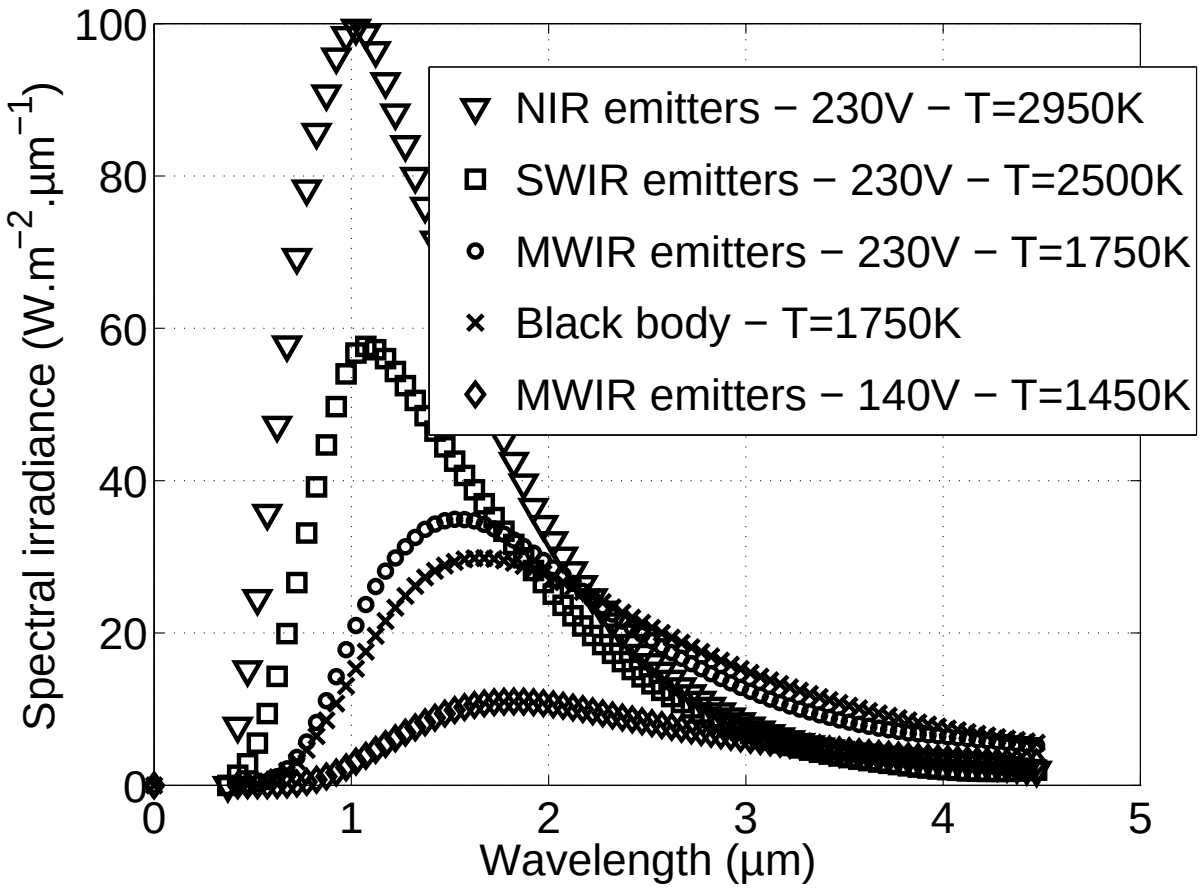

Figure 3. Emitter spectral irradiance as a function of
the emitter wave length, emitter type and emitter lamp temperature.

For the term $\alpha_{\lambda p(\lambda,T_{surf})}$, if we assume the paint opaque, the radiative properties are:

$$\alpha_{\lambda p}(\lambda,T_{surf}) = 1 - \rho^{*}_{\lambda p}(\lambda,T_{surf}) \quad (12)$$

with the spectral reflectance $\rho^{*}_{\lambda p(\lambda,T_{surf})}$ obtained experimentally. If we observe the dynamical reflectance spectra of the painting during the cure (Figure 4), the reflectance spectra do not evolve regularly between the spectrum of the uncured sample to the spectrum of the cured sample. The evolution is more complicated. As the result of the integration of the absorptivity (weighted by the irradiance of emitter), the absorption coefficient of the painting at the top surface $\alpha_{p(T_{surf})}$ is time dependant during the cure (Figure 5), according to both the type of emitter and the cure cycle obtained by manipulating the lamps voltage.

These results show that the absorptivities are lower for the high temperature emitters because their emissions are mostly in the near infrared region where the spectral reflectances of the coatings are higher. This suggests that for a same incident heat flow on the coating surface, low temperature emitters are more effective for curing A-W thermoset coatings (Vechot et al., 2006). For this reason, in this study, we have chosen MWIR type lamps. Nevertheless, optimizing the choice of the lamps based on the entire energy efficiency (from the electrical energy absorbed from the electrical network by the emitter, to the energy absorbed at the surface) is still to be done.

Concerning the sensitivity of the controlled temperature with respect to the model parameters, and as it can be seen from Table 4, the absorption coefficient of the painting α_p is clearly the most important parameter of the model. In this control study, one wants to show the

robustness of the closed loop control of the cure with respect to the most important uncertainties of this model parameters. From a practical point of view for the control, there are two essential questions that are to be answered with this study: is it possible not to use in the model based controller the equations (9), (10) and (11) needed to model the powder coating spectral reflectance at the top surface and the emitter spectral irradiance? Also, is it possible not to use sensors needed to evaluate on-line these two properties? In the proposed control approach, α_p is kept constant according to the color of the painting (0.95 with a black painting, 0.55 with the white painting) and since a closed loop control strategy will be used, α_p must still be seen as an unmeasured (but rather badly estimated) disturbance. The other parameters ε_p and ε_s (used in the boundary conditions (3) and (5)) are also complex to evaluate during any curing cycle since they depends on the infrared flow applied. But they have less impact than α_p and are therefore also assumed as constant values and must also be seen as an unmeasured (or rather badly estimated) disturbance. These properties are not measured on-line.

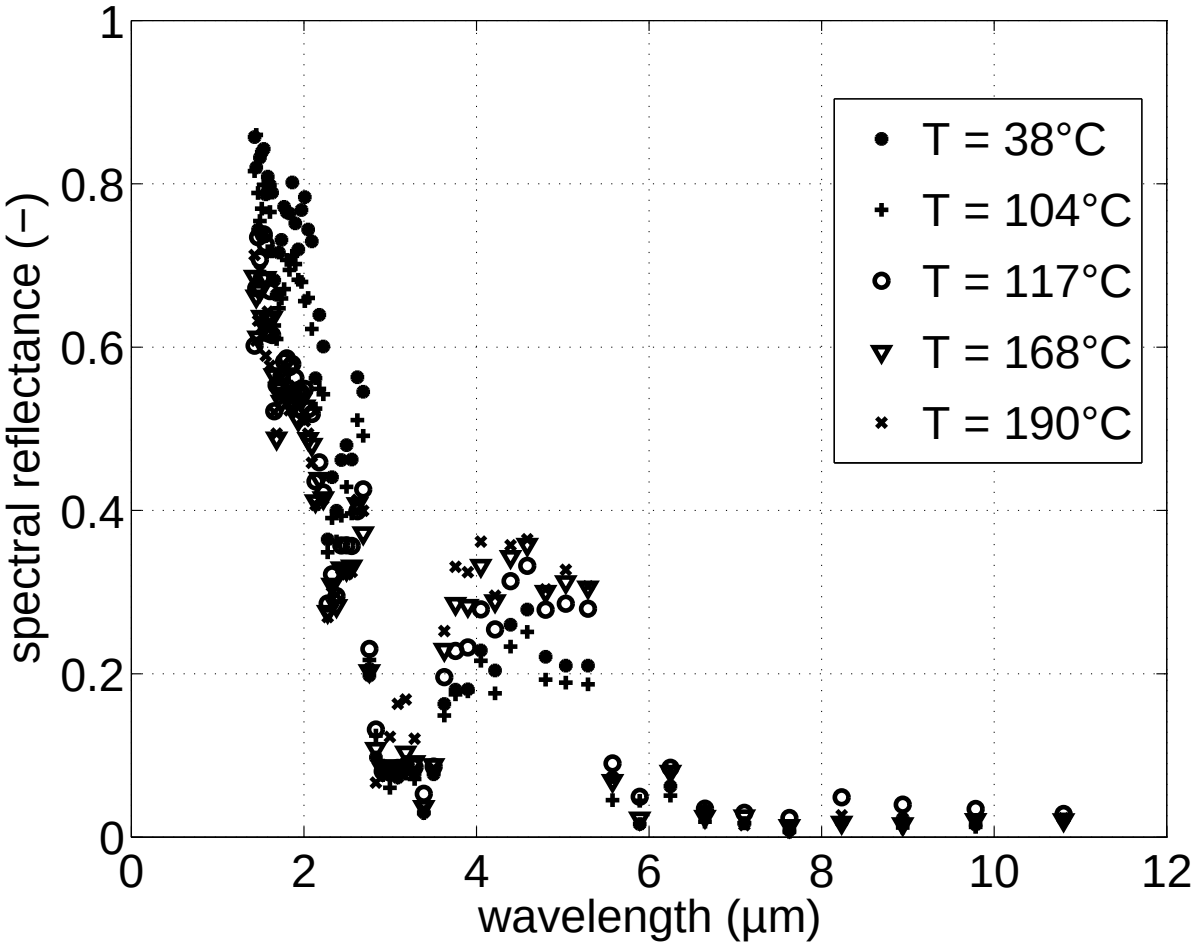

Figure 4. Dynamic spectral reflectance during the cure as a function of the MWIR emitter wave length and the coating temperature.

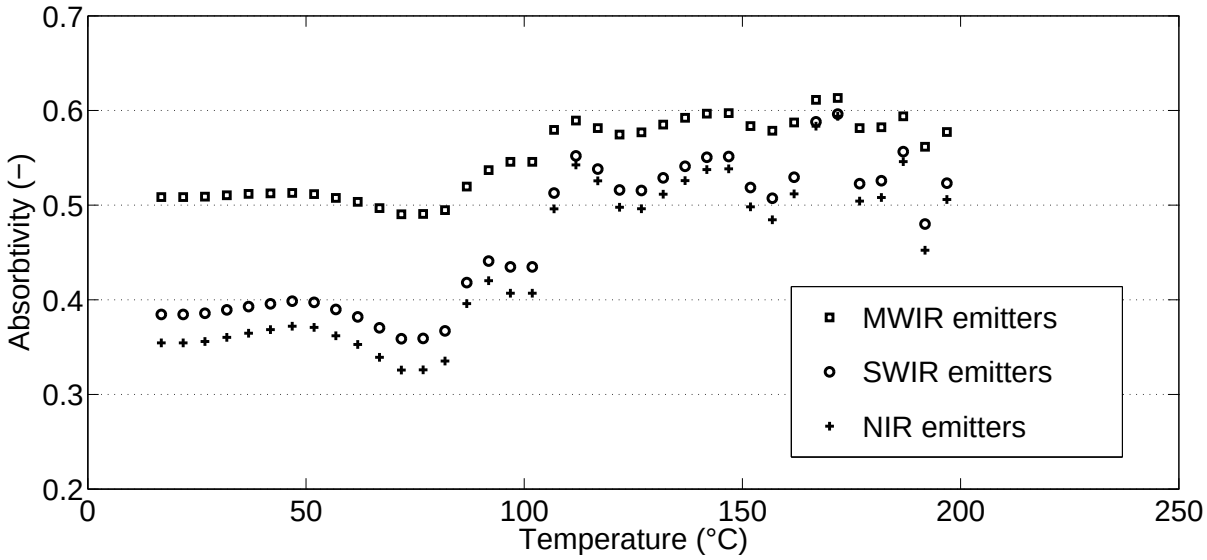

Figure 5. Absorptivity at the surface of the painting as a function of the emitter type and of the coating temperature (cure under 230 V lamps voltage)

Some values of the model parameters are known very easily: the thermo physical properties of the paint were provided by our paint supplier. The thermo physical properties of the substrate are found in the literature. For the chemical conversion, the model is validated and more details about it may be found in (Bombard et al., 2006; Vechot et al., 2006).

This model belongs to a general class of one dimensional non-linear parabolic PDE with boundary control with some uncertain model parameters, and is summarized as follows:

$$(S_{NL})\begin{cases} \dfrac{\partial x_m(\zeta,t)}{\partial t} = F_d(x_m(\zeta,t)) & ,\forall\, \zeta \in \Omega\ ,\ t>0 \\ F_b(x_m(\zeta,t),u(t)) = 0 & ,\forall\, \zeta \in \partial\Omega\ ,\ t>0 \\ x_m(\zeta,0) = x_m^0 & ,\forall\, \zeta \in \Omega \cup \partial\Omega\ ,\ t=0 \\ y_m(t) = C\,x_m(\zeta,t) & ,\forall\, \zeta \in \Omega \cup \partial\Omega\ ,\ t>0 \end{cases} \quad (13)$$

where ζ is the independent space variable, Ω is the spatial domain and $\partial\Omega$ is its boundary, t is the independent time variable. x_m is the model state belonging to an adequate infinite dimensional state space, u is the one dimensional control signal (or manipulated variable), y_m is the model output, F_d and F_b are non-linear operators and C is a linear operator.

3. Control of the painting coating process

3.1. Control objectives

The objective of this part is to show how a MPC may be useful to control on-line such a painting curing process modeled by a PDE system, and how the uncertainty on the unmeasured absorption coefficient at the top surface is well handled by such closed-loop controller. The aim of the experimental study is to evaluate the robustness of the proposed model based controller with respect to model uncertainties; in other words: is it possible to have a simple tuning of both the model and the controller such that the control objectives are

satisfied in spite of the possible change of color of the painting from one experiment to another ? In term of control objective, a prescribed trajectory tracking problem under input and output constraints is specified. This allows comparing the process output obtained with the model based controller with the known prescribed reference behavior y_{ref}.

3.2. Control of PDE systems

In control theory, due to the complexity of the problem, relatively few studies are devoted to the control of processes explicitly characterized by a PDE model, especially in the non-linear case. Indeed, a balance has to be found between the infinite dimensional representation of such model and the possibilities to implement a finite dimensional controller (in order to be technically feasible). Usually, theoretical studies keeping the initial infinite dimensional PDE model are focusing on the existence and unicity of the model solution and also on the solution of a control problem based on this model (Guo et al., 2008; Zong, 2008). Here, since we are interested in the real time control of a non-linear PDE model based process, we are focusing on finite dimensional approaches. There are two ways to implement a finite dimensional controller for an infinite dimensional system: the first one is to keep the infinite dimensional representation of the PDE model, synthesize an infinite dimensional controller, and find a finite approximation of this controller. But since more control tools exist in finite dimension, the second way is most of the time used; it consists in first constructing a finite approximation of the model and synthesizing a finite dimensional controller. Even if various finite dimensional methods are proposed to control such distributed parameter systems, there is no general framework yet. The original PDE model is usually simplified into an ODE model based on: finite differences method, finite volume method, orthogonal collocation method, Galerkin's method, or on modal decomposition. Many results exist with these approximation techniques. In (Christofides and Daoutidis, 1997), nonlinear finite-dimensional output feedback controllers are given for systems of quasi-linear parabolic PDEs with distributed control, for which the eigenspectrum of the spatial differential operator can be partitioned into a finite-dimensional slow one and an infinite-dimensional stable fast complement. In (Baker and Christofides, 2000), a 3 step finite dimensional approximation was used for nonlinear parabolic PDEs with distributed control. More recently, in (Dubljevic et al., 2006), a number of MPC formulations was shown for the distributed control of linear parabolic PDEs with state and input constraints. In (Dubljevic and Christofides, 2006), a modal decomposition technique was used to decompose the system into a finite dimensional (slow) subsystem coupled with an infinite dimensional (fast) subsystem. Various state feedback predictive controllers were then designed. In (Damak, 2007), it was shown how it was possible to design an asymptotic estimator of state and time-varying parameters in the case of a non-linear distributed parameter bioreactor. The structure of the estimator was based on an approximated model of the bioreactor behavior by orthogonal collocation. In (Ravindran, 2007), the optimal boundary feedback stabilization of Navier–Stokes equations using model reduction has been presented. The model reduction was carried out using a combination of proper orthogonal decomposition (POD) and Galerkin projection, and used for the optimal linear quadratic regulator (LQR) synthesis. In (Li and Christofides, 2008), two computationally efficient approaches were presented for the optimal control of diffusion-convection reaction processes described by parabolic PDEs subject to Danckwerts boundary conditions. It was based on reduced-order models combined with a LQR. In (Christofides et al., 2008), an overview of recently developed control methods for PDE based models was presented, with examples on crystallization, aerosol and thermal spray. In (Maidi et al., 2009), a PDE model combined with differential geometry has been applied to compare two boundary control strategies for the temperature of the liquid fluid at the outlet of a heat exchanger. In (Padhiyar and Bhartiya,

2009), the control of the spatial property profile was discussed, since the endpoint itself is a manifestation of the reaction path and a particular path adopted may offer advantages over others. Based on a MPC formulation, a lexicographic optimization was used to prioritize the different sections of the profile when an unachievable target profile was specified. Cascaded continuous stirred tank reactors were used to approximate the model of a pulp digester. In (Aggelogiannaki and Sarimveis, 2008), a radial basis function neural network architecture was used to model the dynamics of distributed parameter systems and was combined with a singular value decomposition to decrease the model order.

3.3. Model Predictive Control

Among the finite dimensional controllers, model predictive control is one of the most popular (Qin and Badgwell, 2003). Model-based predictive control (MBPC) is also named Model Predictive Control, or Receding Horizon Control (RHC). It is a particular class of optimal controller. The idea of model predictive control began in the 1960s (Propoï, 1963). However, a real interest started to emerge in the 1980s after publication of the first papers on identification-command (IDCOM) by (Richalet et al., 1978) and on dynamic matrix control (DMC) (Cutler and Ramaker, 1980). Quadratic DMC (QDMC) by (Cutler et al, 1983) was later able to handle constrained optimization problems. Generalized predictive control (GPC) by (Clarke et al., 1987a, Clarke et al., 1987b) was intended to offer a new adaptive control alternative. Thousands of industrial applications of MPC exist today, for example in the chemical and petrochemical industries: MPC has become the second control paradigm in the history of control after the PID. The first main advantage is that constraints (due to: manipulated variables physical limitations, operating procedures or safety reasons…) may be explicitly specified into this formulation. The second main advantage of MPC is its ability to address long time delays, inverse responses, significant non-linearities, multivariable interactions. In order to control a process with a model, an experimental response of the process may be enough, but for complex systems, it is better to model the process at a fundamental level. The widespread use and success of MPC applications described in the literature attests the improved performance of MPC for control of difficult process dynamics. Many MPC approaches have therefore been proposed along the past three decades, most of them based on a receding-horizon strategy, i.e., at each current sampling instant k the following actions are taken:

- the plant measurements are updated for use in the feedback/feedforward control loop;
- the plant model is used to predict the output response to a hypothetical set of future control sequence;
- a function including the cost of future control actions and future deviations from a reference behavior is optimized to give the best future control sequence;
- the first movement of the optimal control sequence is applied on the process.

These operations are repeated at time $k+1$.

However, if the model exhibits a non-linear behavior, a numerical solution technique must be used to solve this optimal problem. The computational effort varies somewhat because some solution methods require only that a feasible (and not necessarily optimal) solution should be found or that only an improvement should be achieved from time step to time step. Nevertheless, compared to the linear case, the numerical effort is usually important and the algorithm may have some difficulties to find a feasible solution. It may lead to unpredictable consequences for the closed loop performances. The computational effort can be greatly reduced when the system is linearized first in some manner and then the techniques developed for linear systems are employed on-line subsequently. Nevistic (Nevistic, 1997) showed excellent simulation results when a linear time varying (LTV) system approximation is used,

which was calculated at each time step over the predicted system trajectory (Lee and Ricker, 1994). In Zheng works (Zheng, 1997, Zheng, 1998), the non-linear MPC control law was approximated by a linear controller which linearized the non-linear model but assumed that no constraints exist. Therefore, a linear approach may be an interesting solution to have an acceptable computational effort, especially if the sampling period is short. A linearization of the model is used in our study. In (De Temmerman, 2008), the strategy adopted was to use a linearized model instead of a non-linear PDE model in a MPC approach: the control performances were quite similar, while the computational time was decreased by a factor 5. What is more, whereas the non-linear approach was not implementable, the linearized model based control approach was implementable for a drying process featuring a 60 s sampling time.

3.4. Proposed Model Predictive Control formulation for a PDE system

A time-varying linearized PDE model based predictive control algorithm detailed in (Dufour et al., 2003) is used for this research. In previous experimental control of PDE systems (painting drying in (Dufour et al., 2004); pasta drying in (De Temmerman et al., 2009)), it has been shown how this special MPC framework may be used for the control of such PDE system, in spite of the infinite dimensional aspect of the initial model and the non-linearity of the model state. In (De Temmerman et al., 2009), it was shown how MPC led to better performances than PID. In (De Temmerman, 2008), the closed loop control performances using either a off-line non-linear model and a coupled on-line linearized model, or an on-line non-linear PDE model in the MPC approach were quite similar. Whereas the non-linear approach was not implementable, the linearized model based control approach was implementable for a drying process featuring a 60 s sampling time: the computational time was indeed decreased by a factor 5 in the linearized case.
The main ideas of this control algorithm are briefly reminded in this part[1]. To provide an insight into the process, it is necessary to solve the PDE model in finite dimension, and then synthesize a MPC. This controller is designed such that the calculation time is smaller that the small sampling time (a few seconds). This controller is built as a compromise between the small calculation time allowed, and the accuracy of the model used in the on-line model based optimization problem to solve, and the accuracy of the solution found in the iterative procedure. Moreover, unfeasibility of the output constraint is also handled, such that the less bad solution is found.
In this framework, the initial general optimization problem is formulated into the future over a receding horizon *Np*, where the cost function *J* aims to reflect any control problem (trajectory tracking, processing time minimization, energy consumption minimization, …):

$$\min_{u} \quad J(u) = \sum_{j=k+1}^{j=k+Np} \left(h_0(y_{ref}(j), y_p(j), u(j) \right) \quad (14)$$

where k is the actual discrete time ($t=k*Te$), Te is the sampling time, j is the future discrete time index. y_p is the process controlled output that has to follow as best as possible the prescribed reference behavior y_{ref}. This optimization problem can not yet be solved, since it requires the process measures y_p into the future, which is not possible. This issue is handled through an approximation based on the used of the internal model closed loop control structure, where the control u is applied on both the process and the model, and where the feedback term is:

$$e(k) = y_p(k) - y_m(k), \quad \forall k > 0 \quad (15)$$

Assumption 1:
In order to forecast the process output y_p into the future j, it is assumed that the error $e(j)=y_p(j)-y_m(j)$ is constant into the future: $e(j)= e(k)$ is obtained after each update of the measure at time k.

Based on the assumption 1 and on the introduction of the internal model control closed loop structure, the optimization problem is now computationally solvable, since it is based on the feedback term $e(k)$ and on the model response in the future $y_m(j)$ obtained with the model (13):

$$y_p(j) = y_m(j) + e(k), \quad \forall k > 0, \quad \forall j \in [k+1, k+Np] \quad (16)$$

The optimization problem can now be numerically solved:

$$\min_u \quad J(u) = \sum_{j=k+1}^{j=k+Np} \left(h_1(y_{ref}(j), e(k), y_m(j), u(j) \right) \quad (17)$$

Concerning the n general output constraints g_i related to operating conditions, safety, quality, they are formulated as inequality constraints on the measured or estimated output (and the input if needed):

$$g_i(y_p(j), u(j)) \le 0, \quad \forall j \in [k+1, k+Np], \quad \forall i \in I^n = \{1, \dots, n\} \quad (18)$$

Based on the assumption 1 and on the internal model control closed loop structure, the n general output constraints g_i are reformulated, based on the feedback term $e(k)$ and on the model response in the future $y_m(j)$ obtained with the model (13):

$$g_i(e(k), y_m(j), u(j)) \le 0, \quad \forall j \in [k+1, k+Np], \quad \forall i \in I^n = \{1, \dots, n\} \quad (19)$$

The idea of the proposed approach is to transform the initial PDE model based constrained problem into a ODE model based unconstrained problem, such that the time needed to solve the on-line optimization problem is less than the sampling time. Based on this approach, the output constraints g_i are handled in the optimization problem through the penalty term J_{ext}, based on the exterior penalty method (Fletcher, 1987):

$$J_{ext}(u) = \sum_{j=k+1}^{j=K+Np} \left(\sum_{i=1}^{i=n} \left(w_i \max^2 \left(0, g_i(e(k), y_m(j), u(j))\right)\right)\right) \quad (20)$$

where w_i is an adaptive positive defined weight. The advantage is that case where a constraint is not satisfied can be handled. The cost function J and the penalty term J_{ext} are then combined into J_{tot} to formulate the constrained penalized optimization problem:

$$\min_{u} \quad J_{tot}(u) = J(u) + J_{ext}(u) \quad (21)$$

where the manipulated variable u of the process is the constrained optimization argument in the optimization task:

$$\begin{cases} u_{min} \leq u(k) \leq u_{max} \quad , \quad \forall k > 0 \\ \Delta u_{min} \leq u(k) - u(k-1) \leq \Delta u_{max} \quad , \quad \forall k > 1 \end{cases} \quad (22)$$

The constrained optimization argument u is transformed into the unconstrained optimization argument d: it is obtained from a simple hyperbolic transformation of the magnitude and velocity constraints specified for the manipulated variable u (Dufour et al., 2003):

$$u(k) = h_2(d(k) = h_{2.mean} + h_{2.magn} \tanh\left(\frac{d(k) - h_{2.mean}}{h_{2.magn}}\right) \quad , \quad d(k) \in \mathbb{R},\ k > 0 \quad (23)$$

where $h_{2.mean}$ and $h_{2.magn}$ are updated at each time k according to the control action $u(k-1)$ found at the previous discrete time $k-1$:

$$\begin{cases} h_{2.mean} = \dfrac{h_{2.\max} + h_{2.\min}}{2} \\ h_{magn} = \dfrac{h_{2.\max} - h_{2.\min}}{2} \\ h_{2.\max} = \min\left(u_{\max}, u(k-1) + \Delta u_{\max}\right),\ k > 1 \\ h_{2.\min} = \max\left(u_{\min}, u(k-1) + \Delta u_{\min}\right),\ k > 1 \end{cases} \quad (24)$$

The drawback is that this transformation introduces a strong decrease of the sensitivity of the cost function with respect to the optimization argument when u tends to its limits. One of the advantage of such transformation is that the function h_2 (22.) is linear when $u(k)$ tends to $u(k-1)$, i.e. when small changes in the control action is needed. The optimizer argument d is finally used in an on-line penalized unconstrained optimization problem:

$$\min_{d} \quad J_{tot}(d) = J\left(y_{ref}(j), e(k), y_m(j), d(j)\right) + J_{ext}\left(e(k), y_m(j), d(j)\right) \quad (25)$$

Moreover, in order to decrease again the on-line computational time, the argument of the optimization is assumed to be the same into the future:

$$d(j) = d(k), \quad \forall j \in [k+1, k+Np] \quad (26)$$

Widely known and used for its robustness and convergence properties, the Levenberg-Marquardt's algorithm is used here and the optimization argument is determined iteratively at each sample time k using the process measurement (or estimation), the model prediction and the cost function $J_{tot.}$ The drawback is that it allows finding a local solution, which may not be a global solution. Moreover, the hessian required by this method is approximated at the first order.

From a practical point of view, the next step in this problem is to reduce the computational time needed to solve the unconstrained optimization problem during the sampling period. A

linearization method of the non-linear PDE model around a similar non-linear PDE model chosen and computed off-line is used. The system (S_{NL}) is first solved off-line with a particular choice of its input $u(t)=u_0(t)$, which leads to the solution (S_0). The relation between the small input variations Δu, the small state variations Δx_m and small output variations Δy_m about this particular solution (S_0) of the (S_{NL}) may be described by the time varying linearized model (S_{TVL}). More details about the relations between the formulation of (S_{TVL}) and (S_{NL}) may be found in (Dufour et al., 2003). According to the hyperbolic transformation and the linearization, the input Δu of the on-line model (S_{TVL}) is also replaced by the unconstrained parameter Δd (more details may be found in Dufour et al., 2003). Finally, the off-line solved non-linear PDE model and the on-line solved time varying linearized PDE model replace the non-linear model that is initially to be solved on-line.

In order to be able to calculate y_m into the future as required by the cost function (24.), these PDE models are approximated in finite dimension by a discretization technique. Furthermore, the discretization in finite dimension is an essential step for the simulation of the model into the future. In order to decrease the time needed to solve the model used on-line, the number of points in the discretization scheme for (S_{TVL}) and (S_0) is also decreased, such that the finite approximation of the solution of the PDE model is less accurate (in open loop). In the meantime, this approximation is compensated by the closed loop control approach that is still able to reach the specified closed loop performances, like in (Dufour and Touré, 2004).

The final internal model structure with MPC (IMC-MPC) structure is given in Figure 6. The control objective is then to find on-line the variation Δd (hence Δu) of the variable d (hence the manipulated variable u) about a well chosen trajectory d_0 (hence u_0) that improves at each sample time the on line optimization result. The final unconstrained penalized control problem to solve is, at each discrete time k:

$$\min_{\Delta d} J_{tot}(\Delta d) = \sum_{j=k+1}^{j=k+Np} h_3(y_{ref}(j), e(k), y_p(k), \Delta y_m(j, \Delta d(k)), u(\Delta d(k))) \quad (27)$$

with the iterative modified Levenberg Marquardt based algorithm:

$$\Delta d^{l+1}(k) = \Delta d^{l}(k) - \left(\nabla^2 J^{l}_{tot}(k) + \lambda I\right)^{-1} \nabla J^{l}_{tot}(k) \quad (28)$$

where $\nabla J^{l}_{tot}(k)$ and $\nabla^2 J^{l}_{tot}(k)$ are the criteria gradient and criteria hessian with respect to Δd at the iteration l at the time k.

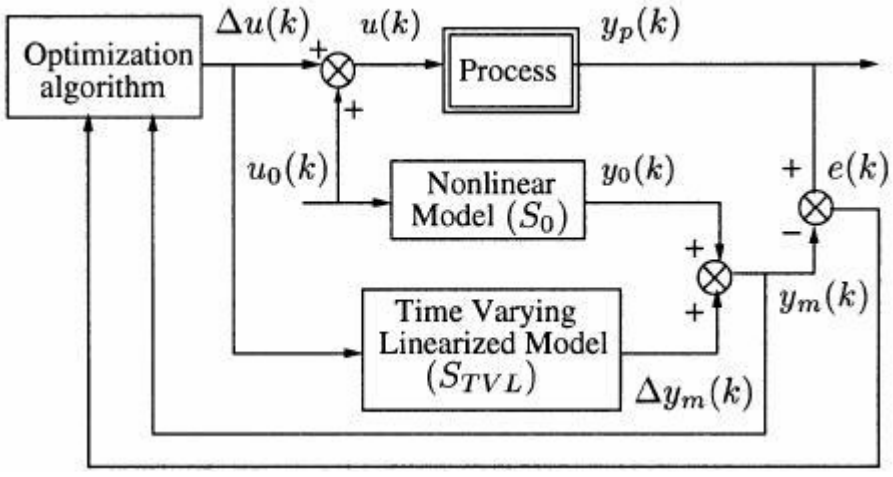

Figure 6. Control structure (Dufour et al., 2003).

Therefore, various approximations or assumptions are introduced at different levels of the control approach (either for the modeling part, or for the search method of the optimal solution) to tune on-line the control action:

1. during the modeling: first, a model is never perfect. Additional assumptions may be specified to obtain an usable model for the model based control approach;
2. during the modeling, some assumed constant parameters may be uncertain, and/or in fact time varying;
3. in order to decrease the on-line computational time, the initial non-linear PDE model is approximated in 2 steps: an non-linear solution is solved off-line, which is the base of the time varying linearized PDE model computed during the on-line optimization task;
4. in order to have an implementable finite dimensional controller, the PDE models are approximated in finite dimension;
5. in order to decrease the on-line computational time, the number of points in the discretization grid used for the resolution of (S_{TVL}) and (S_0) is decreased;
6. in the predictive approach, the error between the process output and the model output is assumed constant (but update at each time k by the last process measurements). It is used as the feedback term;
7. in the iterative optimization, the optimization argument is assumed constant into the future: a step function is sought.
8. in the iterative optimization, the Levenberg-Marquardt based algorithm does not allow to find a global solution, but only a local solution.
9. in the iterative optimization, in the Levenberg-Marquardt based algorithm, the second order term is approximated at the first order.

Since the closed loop model based control approach is based on several assumptions and approximations, it has to present good robustness properties, which must be underlined under simulations first, and under experimental validation.

3.5. Simulation results and discussion

3.5.1 Control software: main features of MPC@CB

A software developed with Matlab[1] is used: MPC@CB[2]. It allows realizing the MPC under constraints of a continuous process. The originality of these codes is first the ease of their use for any continuous SISO process (Single Input Single Output), through the user files (where model equations have to be specified) that are synchronized by few main standards files (where the user has to make few (or no) changes). The model has to be given under the form:

$$\begin{cases} \dot{s} = f(s,u) \\ y = g(s) \end{cases} \tag{29}$$

i.e., there are any number of state variables in this SISO model, it may be linear or not linear, time variant or time invariant, based on ODE and/or PDE.

Another original feature of the software is the straightforward resolution of various model based control problems through different choices:

- MPC for a trajectory tracking problem, with or without the output constraint. The user may specify any reference trajectory;
- MPC to solve an operating time minimization problem, with or without the output constraint;

- in order to study the robustness of the control law, it is easy to introduce, for any model parameter, different values in the model (used in the controller) and in the simulated process. The simulated process and the model may be described by the same (or different) set of equations and by the same (or different) set of parameters;
- possibility to introduce a cascaded process (which input is the output controlled by the software);
- possibility to specify any condition to stop the run before the final time.

The other originality is the method used to develop the codes: it is very easy to introduce new parts in the code, such as:

- MPC with a user defined problem.
- handle SIMO, MISO or MIMO model.
- introduce a software sensor (observer).
- apply the software for a real time application.

Until now, other applications have used MPC@CB: lyophilisation of vials (Daraoui et al., 2008), polymer reactor (Da Silva et al., 2008), painting curing (Flila et al., 2008) and a pasta dryer (De Temmerman, 2008, De Temmerman et al., 2008).

3.5.2. Experimental conditions

Three parameters have been selected to run several experiments in the experimental IR oven:

- the color of the real painting: black or white painting may be used;
- the tuning of the absorption coefficient α_p (Table 6): t is used as a model parameter inside the controller. This will introduce the main model uncertainty. The mean value is not the value of the absorption coefficient for a given painting, but is just the mean value calculated between the value of the absorption coefficients of the black painting and the white painting. According to one of these 3 tuning, we will later refer to the black painting model, the white painting model or the mean model;
- the tuning of the control horizon *Np* in the MPC, since it is the classical main tuning parameter of this kind of controller.

The sampling time is 1s.

3.5.3. Control objectives

In term of control objectives, a prescribed trajectory tracking problem under input and output constraints is specified. This allows comparing the process output obtained with the model based controller with the known prescribed reference behavior y_{ref}. The control objectives are defined as:

- The temperature measure available is considered as the process output: $y_p(t) = T_p(e_p + e_s, t)$. It has to track as best as possible a specified time-dependant reference temperature trajectory $y_{ref}(t)$. Any trajectory may be specified, but since it is usually specified in industrial use, it is defined by a ramp, a constant threshold, a second ramp, and a second constant threshold. Therefore, the cost function involved in the optimization problem (14) is defined as:

$$J(u) = \sum_{j=k+1}^{j=k+Np} \left(y_{ref}(j) - y_p(j) \right)^2 \quad (30)$$

- In order to evaluate the ability of the controller to handle output constraints defined as (18), the process output shall not exceed a maximum value, which is arbitrary chosen equal to less than the second constant value of the reference temperature trajectory:

$$y_p(t) = T_p(0,t) \le y_p^{\max} = 450K \quad (31)$$

  In some sense, the controller has to tune on-line the infrared flow such that the process output tracks the specified solution: the constrained reference y_{ref_const}:

$$y_{ref\_const}(t) = \min(y_{ref}(t), y_p^{\max}) \quad (32)$$

- The infrared flow $\phi_{ir}(t)$, acting as the maniputed variable *u(t)* which is computed by the controller, has to be physically applicable. This is handled by input constraints (22) on the magnitude and velocity of the infrared flow:

$$\begin{cases} 0 \le u(t) \le 23500 W.m^{-2} \\ -10000 W.m^{-2}.s^{-1} \le \dfrac{du(t)}{dt} \le 10000 W.m^{-2}.s^{-1} \end{cases} \quad (33)$$

3.5.4. Experimental results

Several analyses are detailed in this part: first, the impact of the 2 model based controller tuning parameters (the horizon prediction and the modeled absorption coefficient at the top surface) on the closed loop control objectives is presented for the white and for the black painting. Then, the results between white and black paintings are globally compared. In order to compare the experiments, we use two root mean square errors (RMSE):

- the RMSE for the tracking (RMSET) which represents the RMSE between the constrained

reference and the process output, and

- the RMSE for the modeling (RMSEM) which represents the RMSE between the process output and the model output.

They are defined as:

$$\begin{cases} RMSET = \sum_{k=1}^{k=N_k} \left(\sqrt{\frac{(y_{ref\_const}(k) - y_p(k))^2}{N_k}} \right) \\ RMSEM = \sum_{k=1}^{k=N_k} \left(\sqrt{\frac{(y_p(k) - y_m(k))^2}{N_k}} \right) \end{cases} \quad (34)$$

where k is the discrete time t at the current sampled time, and N_k is the number of samples of the considered experiment.

3.5.4.1. Experiments on white paintings

The first set of experiments deals with the white painting. In terms of trajectory tracking, the best experiment is obtained with the white model and a prediction horizon of 12, which leads to the RMSET=3K (Figure 7). The worst experiment is obtained with the black model and for a prediction horizon of 18, which leads to the RMSET=9K (Figure 8). The importance of the modeling for MPC is clearly underlined in these 2 experiments: let us have a look on a time interval where there is no discontinuity in the optimization problem defined on the control horizon. In Figure 7, the tracking is efficient between 40s and 70s; the modeling error e(k) is indeed almost constant and assumption (1) is fulfilled. The modeling into the future is therefore accurate which leads to an efficient tracking. For the same interval, increasing the control horizon from 12 to 18 and choosing the black model makes the tracking less efficient. Indeed, the modeling error e(k) is no more constant (Figure 8) and assumption (1) is no more fulfilled. The modeling is therefore not accurate which leads to a bad tracking.
Concerning the prediction horizon, there is almost for the three models (white, black, mean) a convexity in the tuning (Np=8 or 12) to get the best tracking results (top of Figure 9): if the horizon is too small, the dynamic behavior is not sufficiently presented in the optimizer, whereas a large horizon prediction introduces too many modeling errors into the optimizer.
Concerning the tuning of the painting absorption coefficient in the model used in the MPC, for the same prediction horizon tuning larger than 6, the RMSET with the white model is always better than the one with the mean model, which in turn is better than the RMSET obtained with the black painting model (bottom of Figure 9): the more the color assumed in the model deviates from the real color, the more the tracking error is. Therefore, the structure of the closed loop control impacts the real value of the absorption coefficient of the painting: Indeed, due to this uncertainty, the difference between the process output and the model output (used in the MPC) increases from around RMSEM=10~20K (for the white model) to around RMSEM=70~80K (for the black model) as it can be seen at the bottom of Figure 9. In the meantime, the RMSET increases from the order 3K-5K (for the white model) to 5K-10K (for the black model) as it can be seen at the top of Figure 9. The conclusion is that the use of the white model, based on a constant value for the painting absorption coefficient, leads to a robust closed loop control of the white painting curing in spite of the time dependency of the real painting absorption coefficient.

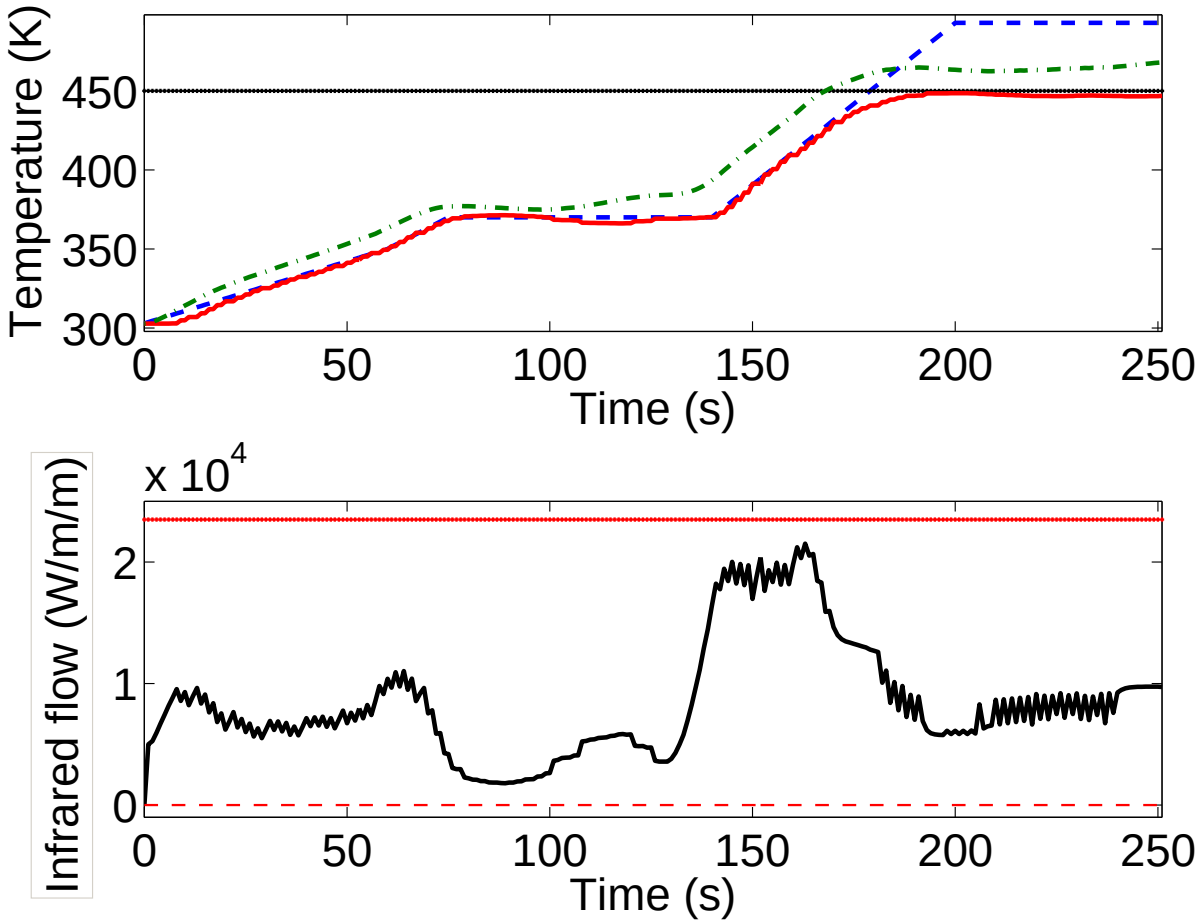

Figure 7. White painting: results with the best RMSET.
Top: Trajectory tracking: reference (--), maximum allowed (+), measure (-), model (-.)
Bottom: Control action: minimum allowed (--), control applied (-), maximum allowed (+).

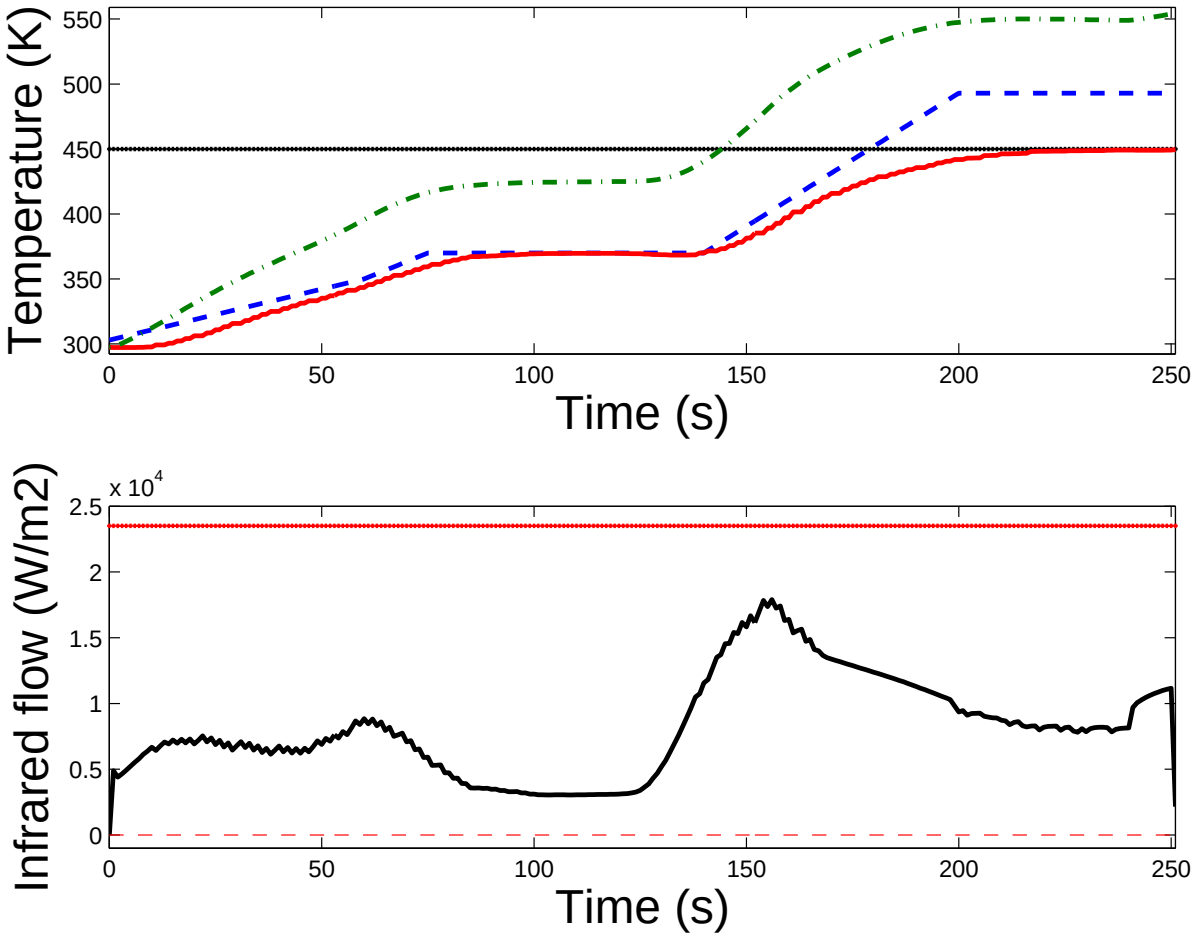

Figure 8. White painting: results with the worst RMSET.
Top: Trajectory tracking: reference (--), maximum allowed (+), measure (-), model (-.)
Bottom: Control action: minimum allowed (--), control applied (-), maximum allowed (+).

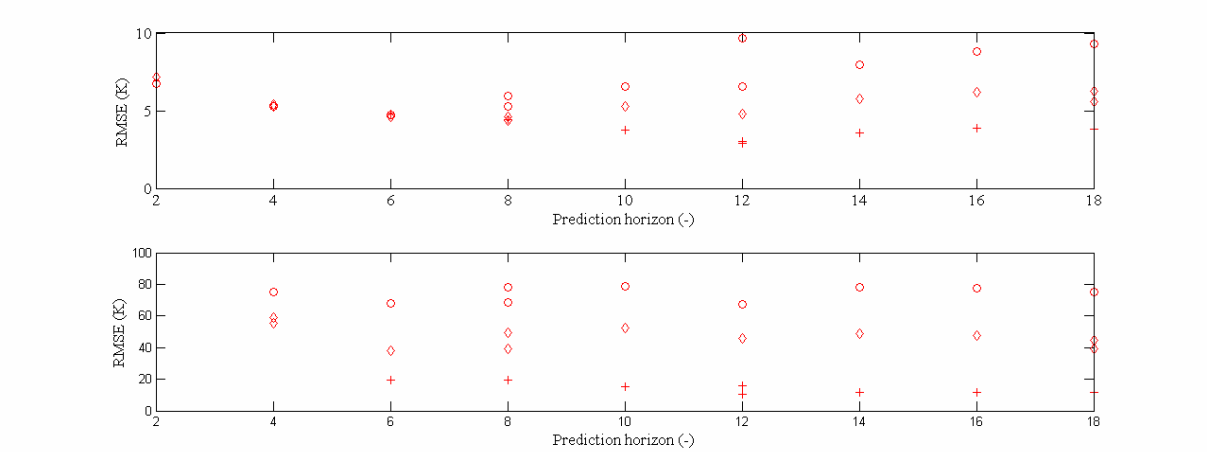

Figure 9. White painting: influence of the tuning of the prediction horizon over the RMSET (top) and RMSEM (bottom). Legend for the painting absorption coefficient tuned in the model: o (black), diamond (mean), + (white).

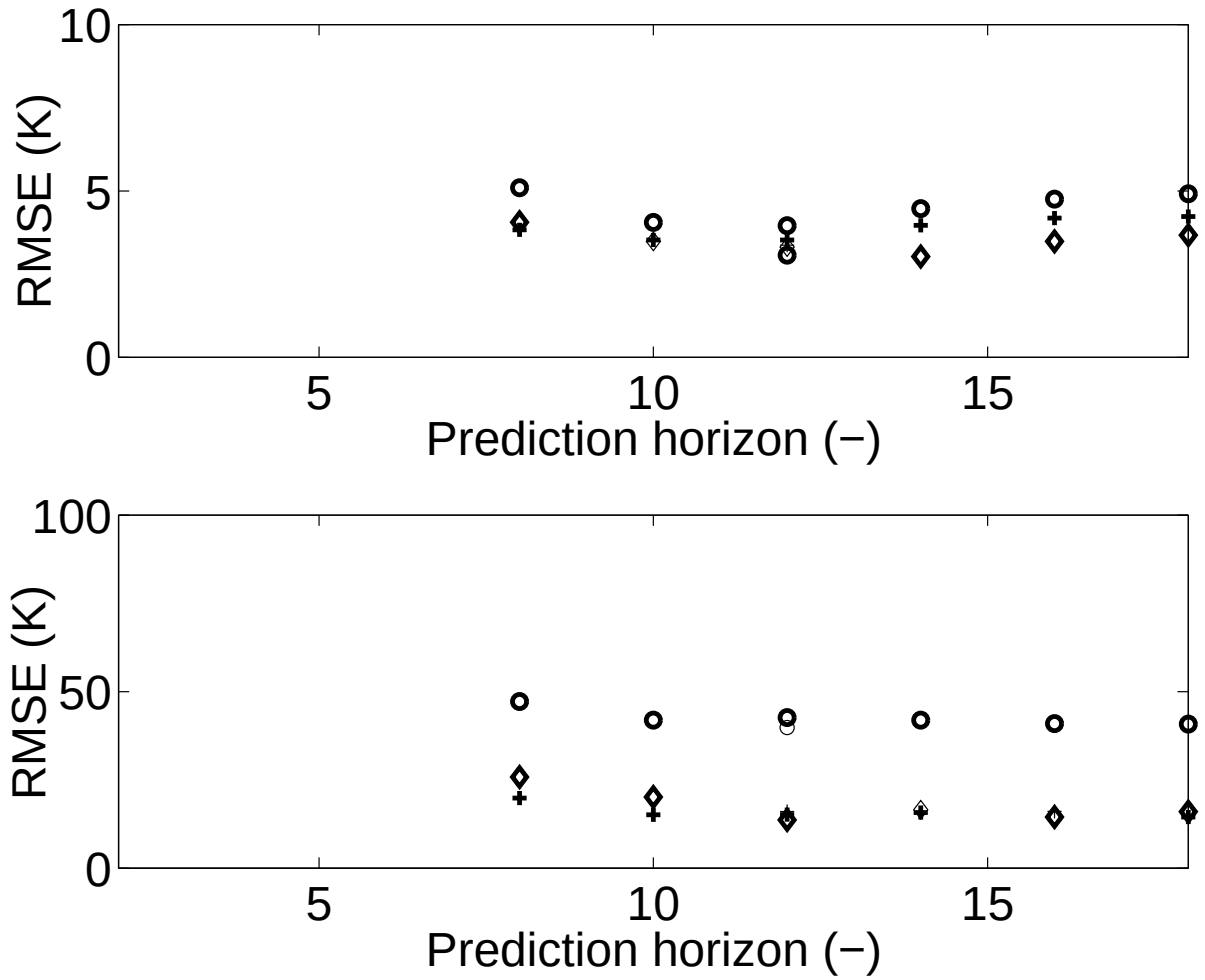

Figure 10. Black painting: influence of the tuning of the prediction horizon over the RMSET (top) and RMSEM (bottom). Legend for the painting absorption coefficient tuned in the model: o (black), diamond (mean), + (white).

3.5.4.2. Experiments on black paintings

The second set of experiments deals with the black painting. In term of trajectory tracking, the best experiment is obtained with the mean model and with a prediction horizon of 14, which leads to the RMSET=3K. The worst experiment is obtained with the black model and with a prediction horizon of 8, which leads to the RMSET=5K. For the three models, there is a convexity in the tuning of the prediction horizon (*Np*=12 or 14) to get the best tracking results (top of Figure 10).

Concerning the tuning of the painting absorption coefficient in the model, for the same prediction horizon tuning, the results obtained with the black model are always the worst, although this is the real color of the painting! That is a real unexpected behavior. Therefore, like for the white painting, the structure of the closed loop control impacts the real value of the absorption coefficient of the painting, whereas this value is still assumed constant in the model. Due to this uncertainty, the difference between the process output and the model output (used in the MPC) increases from around a RMSEM=15~20K (for the mean or white model) to a RMSEM=40~45K (for the black model) as it can be seen at the bottom of Figure 10. In the meantime, the RMSET increases from around 3K-4K (for the mean or white model) to 4K-5K (for the black model). The conclusion is that the black model (based on a constant value for the painting absorption coefficient) is therefore not the best model to use to control

the black painting sample.

3.5.4.3. Global comparison of the experiments

Let us now compare globally the set of experiments:

- According to the RMSET, the MPC is more robust for the black painting than for the white painting, since the uncertainty of the modeled painting absorption coefficient has less impact in closed loop for the black painting than for the white painting. Indeed, for the white painting, from the worst model to the best model, the RMSEM ranges between 80K and 10K, whereas the RMSET ranges from 10K to 3K. For the black painting, from the worst model to the best model, the RMSEM ranges between 45K and 15K, whereas the RMSET ranges from 5K to 3K. The mean of all RMSETs for the white painting is around 6K, whereas the mean of all RMSETs for the black painting is around 4K.
- On one side, the closed loop controller can be seen as the source of the disturbance in the computation of the model into the future time window, since the RMSEM increases between the open loop validation made with a constant emitter infrared flow (Bombard et al, 2008) and the current closed loop results. On the other side, in spite of the RMSEM obtained in closed loop, the controller is again sufficiently robust to tune the infrared flow such that the process output tracks efficiently the prescribed time dependant reference, thus leading to good RMSETs. According to the infrared flow trajectory applied (bottom of Figures 7 and 8), it is obvious that such tracking is not possible manually without automatic feedback.
- Best closed loop control results could be obtained since the best RMSET is always around 3K and since the uncertainty on the measure is 1K. According to the results obtained with the black painting, the tuning of the painting absorption coefficient in the model can not be done a priori based on the constant values obtained off-line and on the choice of the color of the real painting. Since the infrared flow applied in the closed loop control strategy is time-dependant, it impacts a lot the value of the real painting absorption coefficient. This is less obvious for the white painting, since the best results are obtained with the white model. If another color was used, the problem would have to be stated. In order to improve the tracking, it would therefore be of great interest to use observer techniques to estimate on-line the value of the time dependant painting absorption coefficient. This estimate could then be fed on-line in the MPC to decrease the RMSEM and hence improve the control results in terms of RMSET, like in (Edouard et al., 2005). This on-line estimation would be of great interest in order to use this control for a painting of any color, without the need to experimentally identify a priori a constant value for the painting absorption coefficient in the model.

4. Conclusions and perspectives

The experimental model based predictive control of the infrared cure cycle of a powder coating under parameter uncertainty has been tackled. It used a dynamic infinite dimensional model (previously described) aimed at forecasting the temperature during the cure cycle. This partial differential equation model has been approximated in finite dimension to be used in the predictive controller. It has been shown how the absorption coefficient at the surface of the painting sample changes during the cure cycle and affects the radiative behavior of the cure. Experimental closed loop control results of the cure of black and white painting have been shown. According to the results obtained with the black painting, the tuning of the painting

absorption coefficient at a constant value in the model, based on off-line open loop experiments with the real painting, is not easy a priori. Indeed, since the infrared flow applied in this model based closed loop control strategy is usually time-dependant, it impacted a lot the value of the real painting absorption coefficient, which in turn introduced a important modeling uncertainty. This on-line uncertainty had less impact for the cure of the white painting, since the best results have been obtained with the white model. Nevertheless, for both paintings, the specified closed loop performances have been relatively well achieved due to the control structure and the controller robustness. In the control point of view, there is therefore no absolute need of sensor and model to evaluate on-line the powder coating spectral reflectance at the top surface and the emitter spectral irradiance.
Perspectives are first dealing with the use of on-line estimations based on a model based observer to improve the accuracy of the control of the cure for a painting of any color: there would be no need to experimentally identify a priori a constant value for the painting absorption coefficient in the model. This observer would be added into the MPC@CB software, such that the on-line estimate of the absorption coefficient would be fed into the controller as a measured disturbance term. It would be also possible with MPC@CB to use the estimate of the temperature and degree of cure profile to better control the final state of cure, by formulating new constraints on the cure cycle based on these parameters. The second step of future works would be to couple in the MPC the model of cure with a model of other interesting end use properties, such that the gloss. An on-line sensor or estimation of the such property would also be required in the feedback nature of the controller. Thirdly, it would be interesting to do the same control study with other emitter types (NIR and SWIR). With this knowledge, it would be possible to optimize the choice of the emitter type based on the entire energy efficiency (from the electrical energy absorbed from the electrical network by the emitter, to the energy absorbed at the surface), combined with the on-line tuning of the infrared flow emitted by the lamps.

5. References

Lee, S.S., Han, H.Z.Y., Hilborn, J.G., Månson, J.A.E., (1999). Surface structure build-up in thermosetting powder coatings during curing. Progress in Organic Coatings, 36, 79-88.

Véchot, L., Bombard, I., Laurent, P., Lieto, J., (2006). Experimental and modeling study of the radiative curing of a polyester-based coating. International Journal of Thermal Sciences, 45, 86-93.

Weiss, K.D., (1997). Paint and coatings: A mature industry in transition. Progress in Polymer Science, 22(2), 203-245.

Wood, C., (2007). Is my coating cured?. Finishing Today Mag, February, 26-29 http://www.finishingtodaymag.com/CDA/Archives?issue=1860603

Bombard, I., (2007). Contribution à l'étude, au contrôle et à la commande d'un procédé de cuisson radiatif de peintures en poudre. PhD Thesis of the University of Lyon, France.

Bombard, I., Laurent, P., Lieto, J., Jeandel, G., 2008. A model of the infrared cure of powder coatings based on surface absorptivities in-situ measurements. Journal of Coatings Technology and Research, 5(3), 353-363.

Abid, K., Dufour, P., Bombard, I., Laurent, P., 2007. Model predictive control of a powder

coating curing process: an application of the MPC@CB Software, in Proceedings of the 26th IEEE Chinese Control Conference (CCC), Zhangjiajie, China, vol. 2, pp. 630-634.

Degnan, T.F., (1982). Temperature gradients in electron beam cured coatings. Radiation Physics and Chemistry, 19(5), 393-401.

Deans, J.,Kögl, M., (2000). The curing of powder coatings using gaseous infrared heaters: an analytical model to assess the process thermal efficiency. International Journal of Thermal Sciences, 39, 762-769.

Chattopadhyay, D.K., Prasad, P.S.R., Sreedhar, B., Raju, K.V.S.N., (2005). The phase mixing of moisture cured polyurethane-urea during cure. Progress in Organic Coatings, 54(4), 296-304.

Perou, A. L., Vergnaud, J. M., (1997). Correlation between the state of cure of a coil coating and its resistance to liquids. Polymer Testing, 16(1), 19-31.

Salagnac, P., Dutournié, P., Glouannec, P., 2004. Curing of composites by radiation and natural convection in an autoclave. AIChE Journal, 50(12), 3149-3159.

Carr, W.W., Williamson, V.A., McFarland, E.G., Johnson, M.R., (1999). Characterisation infrared absorption by powder coatings on steel panels. Journal of Coatings Technology, 71(889), 71-84.

Bombard, I., Véchot, L., Laurent, P., Lieto, J., (2005). Optimisation de la cuisson sous infrarouge de deux types de peintures en poudre, in Proceedings of the Congrès Français de Thermique SFT, Reims, France.

Papini, M., (1996). Study of the radiative properties of powdered and fibrous polymers, Vibrational Spectroscopy, 11 (1996) 61-68.

Papini, M., (1997). Analysis of the reflectance of polymers in the near- and mid-infrared regions. Journal of Quantitative Spectroscopy and Radiative Transfer, 57(2), 265-274.

Tongsuo, Y., Yang, H., Shujuan, D., Wang, W., Minggui, X., (2002). Infrared reflection of conducting polyaniline polymer coating. Polymer Testing, 21, 641-646.

Ventura, C., Papini, M., (1999). Analysis of the reflectance of granular materials in the near-infrared wavelength range, Journal of Quantitative Spectroscopy and Radiative Transfer, 61(2), 185-195.

Sesták, J., (1984). Thermophysical properties of solids, their measurement and theoretical analysis. Elsevier, Amsterdam.

Bombard, I., Laurent, P., Jeandel, G., Lieto, J., (2006). A model of the cure of powder coatings based on surface absorptivities in-situ measurements, in Proceedings of the Future Coat Conference, New Orleans, LA.

Guo, B.-Z., Wang, J.-M., Yang K.-Y., (2008). Dynamic stabilization of an Euler–Bernoulli beam under boundary control and non-collocated observation. Systems and Control Letters, 57(9), 740-749.

Zong, X., (2008). Optimal control of a non-linear parabolic–elliptic system. Non-linear Analysis, 70(6), 2366-2375.

Christofides, P. D., Daoutidis, P., (1997). Finite-dimensional control of parabolic PDE systems using approximate inertial manifolds. Journal of Mathematical Analysis and Applications, 216, 398-420.

Baker, J., Christofides, P. D., (2000). Finite-dimensional approximation and control of nonlinear parabolic PDE systems. International Journal of Control, 73, 439-456.

Dubljevic, S., El-Farra, N. H., Mhaskar, P., Christofides, P. D., (2006). Predictive control of parabolic PDEs with state and control constraints. International Journal of Robust & Nonlinear Control, 16, 749-772.

Dubljevic, S., Christofides, P.D., (2006). Predictive control of parabolic PDEs with boundary control actuation. Chemical Engineering Science, 61, 6239-6248.

Damak T., (2007). Procedure for asymptotic state and parameter estimation of non-linear distributed parameter bioreactors. Applied Mathematical Modeling, 31, 1293–1307.

Ravindran, S.S., (2007). Optimal boundary feedback flow stabilization by model reduction. Computer Methods in Applied Mechanics and Engineering, 196, 2555–2569.

Li, M., Christofides, P.D., (2008). Optimal control of diffusion-convection-reaction processes using reduced-order models. Computers and Chemical Engineering, 32, 2123-2135.

Christofides, P.D., El-Farra, N., Li, M., Mhaskar, P., (2008). Model-based control of particulate processes. Chemical Engineering Science, 63, 1156-1172.

Maidi, A., Diaf M., Corriou, J.P., (2009). Boundary geometric control of a counter-current heat exchanger. Journal of Process Control 2009,19(2), 297-313.

Padhiyar, N., Bhartiya S., (2009). Profile control in distributed parameter systems using lexicographic optimization based MPC. Journal of Process Control 2009, 19(1), 100-109.

Aggelogiannaki, E., Sarimveis, H., (2008). Non-linear model predictive control for distributed parameter systems using data driven artificial neural network models. Computers and Chemical Engineering, 32, 1225-1237.

Qin, S.J., Badgwell, T.A. (2003). A survey of industrial model predictive control technology. Control Engineering Practice 11(7), 733-764.

Propoi, A. I., (1963). Use of linear programming methods for synthesizing sampled-data automatic systems. Automat. Rem. Control, 24(7), 837–844.

Richalet, J., Rault, A., Testud, J. L., Papon, J., (1978). Model predictive heuristic control: Applications to industrial processes. Automatica, 14, 413-428.

Cutler, C. R., Ramaker, B. L., (1980). Dynamic Matrix Control: a computer control

algorithm. In Proceedings of the Joint Automatic Control Conference, San Francisco, CA

Cutler, C., Morshedi, A., Haydel, J. (1983). An industrial perspective on advanced control, in AICHE annual meeting, Washington, DC.

Clarke, D. W., Mohtadi, C., Tuffs, P. S., (1987). Generalized predictive control. Part 1: The basic algorithms. Automatica, 23(2), 137-148.

Clarke, D. W., Mohtadi, C., Tuffs, P. S., (1987). Generalized predictive control. Part 2: Extensions and interpretations. Automatica, 23(2), 149-160.

Nevistic, V., (1997). Constrained control of non linear systems. PhD thesis, ETH-Swiss Federal Institute of Technology, Zürich, Switzerland.

Lee, J. H., Ricker, N. L., (1994). Extended Kalman filter based non-linear model predictive control. Industrial and Engineering Chemistry Research, 33 (6), 1530–1541.

Zheng, A., (1997). A computationally efficient non linear model predictive control algorithm, in Proceedings of the American Control Conference, Albuquerque, NM.

Zheng, A., (1998). Non linear model predictive control of the Tennessee–Eastman process, in Proceedings of the American Control Conference, Philadelphia, PA.

De Temmerman, J., (2008). Development of a drying model for the moisture concentration in pasta with control design of the drying air properties. PhD Thesis of the Katholieke Universiteit Leuven, Belgium, ISBN 978-90-8826-057-5.

Dufour, P., Touré, Y., Blanc, D., Laurent, P., (2003). On non-linear distributed parameter model predictive control strategy: On-line calculation time reduction and application to an experimental drying process. Computers and Chemical Engineering, 27(11), 1533-1542.

De Temmerman, J., Dufour, P., Nicolaï, B., Ramon, H., (2009). MPC as control strategy for pasta drying processes. Computers and Chemical Engineering 2009, 33(1), 50-57.

Daraoui, N., Dufour, P., Hammouri, H., Hottot, A., (2008). Optimal operation of sublimation time of the freeze drying process by predictive control: Application of the MPC@CB Software, in Proceedings of the 18th European Symposium on Computer Aided Process Engineering (ESCAPE), Lyon, France, pp. 453-458.

Da Silva, B., Dufour, P., Othman, N., Othman, S., (2008). Model predictive control of free surfactant concentration in emulsion polymerization, in Proceedings of the 17th IFAC World Congress, Seoul, South Korea, Paper 1693, pp. 8375-8380.

Flila, S., Dufour, P., Hammouri, H., (2008). Optimal input design for on-line identification: A coupled observer-MPC approach, in Proceedings of the 17th IFAC World Congress, Seoul, South Korea, Paper 1722, pp. 11457-11462.

Edouard, D., Dufour, P., Hammouri, H., (2005). Observer based multivariable control of a catalytic reverse flow reactor: Comparison between LQR and MPC approaches. Computers and Chemical Engineering, 29(4), 851-865.